The added value of chest high-resolution CT findings of Corona Virus Disease 2019 in predicting severity of disease

Jie Zhou
Department of Radiology, Longgang District People's Hospital of Shenzhen City, The Third Affiliated Hospital (Provisional) of The Chinese University of Hong Kong

Jie Cao
Department of Radiology, Jiujiang First People's Hospital

Ziyun Xiang
Department of Radiology, Longgang District People's Hospital of Shenzhen City, The Third Affiliated Hospital (Provisional) of The Chinese University of Hong Kong

Hanshou Cai
Department of Radiology, Longgang District People's Hospital of Shenzhen City, The Third Affiliated Hospital (Provisional) of The Chinese University of Hong Kong

Yuhui Zhu
Department of Radiology, Longgang District People's Hospital of Shenzhen City, The Third Affiliated Hospital (Provisional) of The Chinese University of Hong Kong

Heng Zhang
Department of Radiology, Longgang District People's Hospital of Shenzhen City, The Third Affiliated Hospital (Provisional) of The Chinese University of Hong Kong

Xu Huang
Department of Radiology, Longgang District People's Hospital of Shenzhen City, The Third Affiliated Hospital (Provisional) of The Chinese University of Hong Kong

Wanling Ma (mawanling321@163.com)
Department of Radiology, Longgang District People's Hospital of Shenzhen City, The Third Affiliated Hospital (Provisional) of The Chinese University of Hong Kong

Keywords: chest thin-section high-resolution CT, COVID-19, early screening, predicting disease severity

Posted Date: March 17th, 2020

DOI: https://doi.org/10.21203/rs.3.rs-17701/v1

Abstract

The aim of this study was to retrospectively analyze chest thin-section high-resolution CT (HRCT) findings for 32 patients with Corona Virus Disease 2019 (COVID-19) and clarify the correlation between CT data and laboratory results. 30 patients presented with abnormal initial CT scans. Of 30 patients, COVID-19 showed the involvement of bilateral lungs in 24 (80%), involvement of more than two lobes in 24 (80%), ground-glass opacities without consolidation in 27 (90%), ground-glass opacities with consolidation in 23 (76.7%), opacities with irregular intralobular lines in 26 (86.7%), opacities with round morphology in 25 (83.3%), and peripheral distribution in 30 (100%). Pleural effusion or mediastinal lymphadenopathy was relatively rare manifestations. Rapidly progression of the disease demonstrated by increasing number and range of ground glass opacities and appearance of consolidations at follow-up CT images in two patients. The CT lung severity score and No. of lobes involved were negatively correlated with lymphocyte count(r=-0.363, P=0.041; r=-0.367, P=0.039, respectively). Chest HRCT of COVID-19 predominantly manifests multiple, round, ground glass opacities with irregular intralobular lines, and peripheral distribution of bilateral lungs. HRCT is a potential tool for early screening, assessing progress, and predicting disease severity of COVID-19.

Authors Jie Zhou and Jie Cao contributed equally to this work and are co-first authors.

Introduction

An acute respiratory disease caused by a new corona virus, first broken out in Wuhan City, Hubei Province of China, is rapidly spreading around the world since December 20191,2. On February 11, 2020, the World Health Organization (WHO) officially named this disease as Corona Virus Disease 2019 (COVID–19). On the same day, International Committee on Taxonomy of Viruses (ICTV) named this new corona virus as SARS-CoV–2,

i.e. 2019 novel coronavirus (2019-nCoV)3. The pathogen was classified in the beta genus4 and first isolated in the Wuhan seafood market5. Like the severe acute respiratory syndrome (SARS), the human-to-human transmission among persons exposed to COVID–19 infection has been documented recently6,7. The inhalation droplets or aerosol transmission and contact transmission of COVID–19 have been confirmed; and faecal-oral transmission has yet to be further confirmed7. The incubation period of COVID–19 ranges

from 1 to 14 days, usually from 3 to 7 days8. Therefore, the 14-day medical observation or quarantine period would be the best management for exposed persons. With the spread of this coronavirus, COVID–19 has been found in many cities of China and abroad9. International coordination and cooperation will be essential to control the spread of the COVID–19 and to prevent the explosive super-transmission events.

Based on current experience, pulmonary imaging appearances occur earlier than clinical symptoms10. Patchy/punctate ground glass opacities are the most common manifestations of COVID–19

pneumonia10–12. Chest digital radiography has a limited effect in showing ground glass opacities due to its overlapping imaging characteristics. Similar to the CT findings of SARS11, ground glass opacities of COVID–19 may be accompanied by interlobular septal thickening and irregular intralobular lines. These imaging changes manifest pathologically by interstitial and intra-alveolar edema, mild interstitial infiltration with inflammatory cells, and vascular congestion13. High resolution CT (HRCT) is the most sensitive imaging technique for exhibiting early lung changes such as punctate ground glass opacities14. Thin-section CT imaging is more sensitive to exhibit interlobular and intralobular septal changes than thick-slice CT images and provides more detailed radiological features15.

To the best of our knowledge, there are a few reports focused on the imaging features of the COVID–19 10,11. Therefore, we analyzed the HRCT imaging findings of 32 patients with COVID–19 in this study. The aim of present study was to demonstrate the pulmonary characteristic manifestations of COVID–19 for early identification of this communicable disease and early isolation of patients, which enabled early implementation of public health surveillance, control and response to the epidemic.

Results

Clinical and pathological characteristics of patients

20 males and 12 females were included in the study (age ranged from 19 to 80 years; mean age, 49.09±16.89 years). 10 patients had a history of residence in or travel to Wuhan, while 17 patients had exposed to infected patients of COVID–19. Some of them were family cluster cases. The clinical symptoms of COVID–19 included fever (84.38%), cough (59.38%), fatigue (15.63%), headache (18.75%), muscle soreness (9.38%), and nausea (15.63%). The clinical characteristics of patients were summarized in Table 1. White blood cell counts of most COVID–19 patients (84.4%) were normal and the rest (15.6%) were lower. Lymphocyte counts of 16 COVID–19 patients (62.5%) were lower and the rest (37.5%) were normal. Neutrophil counts of most COVID–19 patients (93.8%) were normal and the rest (6.2%) were higher or lower. The laboratory characteristics of patients were summarized in Table 2.

Initial CT images characteristics

Among 32 COVID–19 patients, 2 cases had the entirely normal initial CT images and the remaining 30 cases had abnormal CT findings. Abnormal CT findings were summarized in Table 3. The lesions involved bilateral lung in 24 cases (80%) and unilateral lung in 6 cases (20%). Among 30 cases with abnormal CT findings, 6 cases (20%) had one lobe involved and the rest (80%) had multiple lobes involved. The upper lobe was affected in 19 cases (63.3%, right) and 21 cases (70%, left). The right middle lobe was affected in 15 cases (50%). The lower lobe was affected in 24 cases (80%, right) and 27 cases (90%, left). All patients with abnormal CT findings exhibited ground glass opacities with or without consolidation. 27 cases (90%) showed pure ground glass opacities (without consolidation) and 23 cases (76.7%) exhibited ground glass opacities mixed consolidation. Most ground glass opacities were round

(25/30, 83.3%) or flaky (11/30, 36.7%); a few ground glass opacities were semilunar (6/30, 20%). There was no lesion showing only consolidation (without ground glass opacities). The lesions of all patients involved the peripheral field of lung, especially the subpleural region (Fig. 1). Some of them accompanied with central region involved (13/30, 43.3%). Notably, the vascular bundles congestion and intralobular lines within ground glass opacities could be seen in most patients (26/30, 86.7%) (Fig. 2). The accompanying signs of COVID−19 included mediastinal lymphadenopathy (1/30, 3.3%) and pleural effusion (2/30, 6.7%).

Follow-up Chest CT

Three patients underwent follow-up chest CT scan during the study date range, one of whom performed two follow-up CT scans. The time interval between initial CT and follow-up CT scans was 2 days. The initial CT and follow-up CT revealed no pulmonary lesions in 1 patient. The other 2 patients showed rapidly progression that manifested by increasing number and range of ground glass opacities and pulmonary lesions (Fig. 3).

Correlation analyses between the CT data and laboratory data

The number of lobes involved showed a statistically negative correlation with lymphocyte count (r = −0.367, P = 0.039) (Table 4, Fig. 4a). The CT lung severity score was negatively correlated with lymphocyte count (r = −0.363, P = 0.041) (Table 4, Fig. 4b). No significant correlation was found between the number of lobes involved or the CT lung severity score and white blood cell count (r = −0.197, P = 0.281; r = −0.135, P = 0.460; respectively) (Table 4).

Discussion

According to the guideline revised by National Health Commission of China (Trial version 6), the confirmed diagnosis of COVID−19 should be based on the positive 2019-nCoV detection. However, the positive imaging manifestation is one of the indispensable clinical diagnostic criteria. Moreover, the sensitivity of 2019-nCoV nucleic acid detection is poor despite its high specificity16. Therefore, it is of great significance to accurately recognize the imaging features of COVID−19 for its rapid screening and early diagnosis. Chest HRCT with thin-section is currently considered to be one of the most effective tools to early screening and accurate assessment for COVID−19 owing to its high sensitivity and convenience.

The present study demonstrated that: (1) Most COVID−19 patients had bilateral lung involvement (24/30, 80%) and more than two lobes involvement (24/30, 80%). (2) Multiple ground glass opacities were pulmonary characteristic manifestations of COVID−19. All COVID−19 patients with abnormal CT findings demonstrated either pure ground glass opacities (27/30, 90%) or ground glass opacities with consolidation (23/30, 76.7%). Numerous irregular intralobular lines were visible within the ground glass

opacities in most patients (26/30, 86.7%). (□) ground glass opacities usually appeared as round (25/30, 83.3%) or flaky (11/30, 36.7%) morphology. (□) Pulmonary lesions of COVID–19 mainly located in the peripheral region of lung, especially the subpleural regions. In addition, some accompanying signs were occasionally found including mediastinal lymphadenopathy (3.3%) and pleural effusion (6.7%). Two patients in present study, whose family members were confirmed as COVID–19, had typical COVID–19 CT findings but negative findings in the first two etiological testings. They were finally confirmed as COVID–19 by the third etiological testing. For these patients with typical COVID–19 CT findings, it is essential to take early isolation and medical observation if they are living in or traveling from areas of the COVID–19 outbreak, even if they have the negative 2019-nCoV test.

2019-nCoV is highly homologous to the previous SARS-CoV2,17. The pathological features of COVID–19 are greatly similar to those seen in SARS and Middle Eastern respiratory syndrome (MERS) coronavirus infection18,19. Type □ alveolar epithelium is the target cell of the coronavirus. Similar to SARS CoV, 2019-nCoV adheres firstly to alveolar epithelium in peripheral lobules and then damages alveolar walls causing interstitial and intra-alveolar edema, interstitial inflammatory infiltration, dominated by lymphocytes13,20. These pathological changes simultaneously involve multiple adjacent lobules. HRCT images appear as single or multiple ground glass opacities locating peripheral lung fields accordingly. With the progress of disease, multiple patchy ground glass opacities increase and fuse to round or flaky lesions without the distribution of the pulmonary segments. Lung involvements with a peripheral predominance of ground glass opacities are also the primary CT findings of SARS21 and MERS22. On CT images, pleural effusions could be found in few patients with SARS or MERS, but lymphadenopathy could not be seen in any patient23,24. The absence of pleural effusions in most patients was also characteristic of COVID–19 in our study. According to previous research, early onset of pleural effusion with a higher pulmonary CT scores was a sign of poor prognosis25. Focal ground glass opacities and consolidations located in peripheral subpleural fields rapidly progressed to almost the whole lung and were responsible for ensuing acute respiratory distress syndrome (ARDS)25. ARDS commonly occurred in SARS and MERS26. Therefore, COVID–19 patient with pleural effusion and a short incubation period should be given adequate attention and aggressive treatment to prevent rapid progression even to ARDS.

2019-nCoVs distribute over respiratory mucosa, infect other cells, cause a cytokine storm in the body, produce a chain of immune responses, and generate changes in immune cells and peripheral white blood cells. Noticeably, 2019-nCoV mainly attacks lymphocyte, particularly T lymphocyte, thus, a decrease in lymphocyte count is a common laboratory test finding of COVID–19 infection. Degree of lymphocytopenia might be a critical predictive factor associated with disease severity and mortality7. The present study demonstrated the negative correlation between the number of lobes involved or the CT lung severity score and lymphocyte count. The CT lung severity score and the number of lobes involved may be the surrogate biomarkers in predicting disease severity of COVID–19.

There were several limitations in our study. First, the sample size of the present study was relatively small. Only 3 cases had followed-up CT scans. The progressions and outcomes of COVID–19 have not been accurately assessed. Second, our cases were all adults. The CT findings of COVID–19 in children

have not been evaluated. Third, because not all of cases were from Wuhan, our results may be incomprehensive.

In conclusion, the pulmonary CT of COVID–19 predominantly demonstrates multiple ground glass opacities, with a preference for bilateral lungs involvement in peripheral regions. Pleural effusion and mediastinal lymphadenopathy are rare imaging manifestations in COVID–19. Identifying these imaging characteristics in patients living in or having travelled to Wuhan or other epidemic areas can be helpful for early and timely diagnosis of COVID–19. The CT lung severity score and the number of lobes involved have the negative correlation with lymphocyte count. Thin-section HRCT may play an important role in predicting disease severity of COVID–19.

Materials And Methods

This retrospective study was granted by the Institutional Ethical Review Board of our hospitals with a waiver of informed consent.

Clinical data and CT Protocol

32 patients with confirmed COVID–19 presented to two hospitals in two cities underwent plain chest CT during January 17 to February 6, 2020. Nine patients were imaged with 1.25-mm slice thickness on a GE optima 540 CT scanner (GE Medical Systems, Milwaukee, Wis). Twenty-three patients were imaged with 0.625-mm slice thickness on a GE optima 520 Pro CT scanner (GE Medical Systems, Milwaukee, Wis) and a Siemens SOMATOM CT scanner (Siemens Healthineers, Erlangen, Germany). All patients were supine, head advanced, and end-inspiration breathhold during the examination.

Clinical data were collected including age, sex, symptoms, travel and exposure history. Peripheral blood routine test data were also collected. Notably, case selection of this study was consecutive in the two hospitals separately.

CT images analysis

All chest CT images were gathered and reviewed by two radiologists with more than 8 years' experience in thoracic imaging diagnosis independently. Final decisions were reached by consensus. When the result was inconsistent, the final decision was made by a chief radiologist with 22 years' experience in imaging diagnosis.

The CT features of all the 32 patients were evaluated as follows: (□) Pulmonary lesions: The location, morphology, number and density of the lesions were analyzed. Moreover, the number of lobes involved by lesions was also analyzed. (□) Accompanying signs: The presence of pleural effusion, mediastinal lymphadenopathy (the lymph node in size of ≥10 mm in short-axis dimension). (□) The CT lung severity score: Based on tracheal carina and inferior pulmonary veins, each lung was divided into three zones

including upper middle, and lower zones. For each lung zone, the severity score ranged from 0 (normal) to 4. The 0–4 represented normal (0%), minimal (1%–25%), mild (26%–50%), moderate (51%–75%), or severe (76%–100%) respectively. The sum of scores afforded total lung involvement (maximal CT score was 24 for both lungs). (□) Progression of disease: 3 patients underwent a follow-up chest CT during our study time window. These images were assessed to the change and progression over time.

Statistical analysis

Statistical analysis was performed using SPSS software for Windows (version 17.0, SPSS Inc., Chicago, IL). The Pearson correlation test was executed to assess the correlation between the blood test data and CT data. The tests were two-tailed, and *P*-values <0.05 were considered to indicate statistically significant difference.

Data Availability Statement: The authors declare data of this manuscript is authentic and reliable, and can provide a URL or other unique identifier in the manuscript upon any requirement from the reader.

References

1. Perlman S. Another Decade, Another Coronavirus. *N Engl J Med* **382,** 760-2 (2020).
2. Zhu N, et A Novel Coronavirus from Patients with Pneumonia in China, 2019. *N Engl J Med* **382,** 727-33 (2020).
3. Mattiuzzi C, Lippi Which lessons shall we learn from the 2019 novel coronavirus outbreak? *Ann Transl Med* **8,** 48 (2020).
4. Wei JP, et 2019 Novel Coronavirus (COVID-19) Pneumonia: serial Computer Tomography Findings. *Korean J Radiol.* https://doi.org/10.3348/kjr.2020.0112 (2020).
5. Bajema KL, et Persons Evaluated for 2019 Novel Coronavirus- United States, January 2020. *MMWR Morb Mortal Wkly Rep* **169,** 166-70 (2020).
6. Yoon SH, et Chest Radiographic and CT Findings of the 2019 Novel Coronavirus Disease (COVID-19): Analysis of Nine Patients Treated in Korea. *Korean J Radiol*. https://doi.org/10.3348/kjr.2020.0132 (2020).
7. Chan JF, et A familial cluster of pneumonia associated with the 2019 novel coronavirus indicating person-to-person transmission: a study of a family cluster. *Lancet* **395,** 514-23 (2020) .
8. Lin X, Gong Z, Xiao Z, Xiong J, Fan B, Liu Novel Coronavirus Pneumonia Outbreak in 2019: Computed Tomographic Findings in Two Cases. *Korean J Radiol* **21,** 365-8 (2020) .

9. Wang C, Horby PW, Hayden FG, Gao A novel coronavirus outbreak of global health concern. *Lancet* **395,** 470-3 (2020) .
10. Pan Y, et Initial CT findings and temporal changes in patients with the novel coronavirus pneumonia (2019-nCoV): a study of 63 patients in Wuhan, China. *Eur Radiol*. https://doi.org/10.1007/s00330-020-06731-x (2020)
11. Chung M, et CT Imaging Features of 2019 Novel Coronavirus (2019-nCoV). *Radiology*. https://doi.org/10.1148/radiol.2020200230 (2020).
12. Huang C, et Clinical features of patients infected with 2019 novel coronavirus in Wuhan, China. *Lancet* **395,** 497-506 (2020).
13. Ketai L, Paul NS, Wong Radiology of severe acute respiratory syndrome (SARS): the emerging pathologic-radiologic correlates of an emerging disease. *J Thorac Imaging* **21,** 276-83 (2006).
14. Wong CK, Lai V, Wong Comparison of initial high resolution computed tomography features in viral pneumonia between metapneumovirus infection and severe acute respiratory syndrome. *Eur J Radiol* **81,** 1083-7 (2012).
15. Xing ZH, et Thin-section computed tomography detects long-term pulmonary sequelae 3 years after novel influenza A virus-associated pneumonia. *Chin Med J (Engl)* **128,** 902-8 (2015) .
16. Tan WJ, et A novel coronavirus genome identified in a cluster of pneumonia cases-Wuhan, China 2019-2020. *China CDC Weekly* **2,** 61-2 (2020).
17. Wan Y, Shang J, Graham R, Baric RS, Li Receptor recognition by novel coronavirus from Wuhan: An analysis based on decade-long structural studies of SARS. *J Virol*. https://doi.org/10.1128/JVI.00127-20 (2020).
18. Ding Y, et The clinical pathology of severe acute respiratory syndrome (SARS): a report from China. *J Pathol* **200,** 282-9 (2003).
19. Lee KS. Pneumonia Associated with 2019 Novel Coronavirus: Can Computed Tomographic Findings Help Predict the Prognosis of the Disease? *Korean J Radiol* **21,** 257-8 (2020).
20. Xu Z, et Pathological findings of COVID-19 associated with acute respiratory distress syndrome. *Lancet*. https://doi.org/10.1016/S2213-2600(20)30076-X (2020)
21. Wong KT, et Thin-Section CT of Severe Acute Respiratory Syndrome: Evaluation of 73 Patients Exposed to or with the Disease. *Radiology* **228**, 395-400 (2003).
22. Ajlan AM, Ahyad RA, Jamjoom LG, Alharthy A, Madani Middle East Respiratory Syndrome Coronavirus (MERS-CoV) infection: chest CT findings. *AJR Am J Roentgenol* **203,** 782-7 (2014).
23. Müller NL, Ooi GC, Khong PL, Nicolaou S. Severe Acute Respiratory Syndrome: Radiographic and CT Findings. *AJR Am J Roentgenol* **181,** 3-8 (2003).
24. Das KM, Lee EY, Langer RD, Larsson Middle East Respiratory Syndrome Coronavirus: What Does a Radiologist Need to Know? *AJR Am J Roentgeno* **206,** 1193-201 (2016).
25. Das KM, et CT Correlation With Outcomes in 15 Patients With Acute Middle East Respiratory Syndrome Coronavirus. *AJR Am J Roentgeno* **204,** 736-42 (2015).

26. Dyall J, et Middle East Respiratory Syndrome and Severe Acute Respiratory Syndrome: Current Therapeutic Options and Potential Targets for Novel Therapies. *Drugs* **77,** 1935-66 (2017).

Declarations

Acknowledgments: None.

Authors contributions: J. Z. designed and wrote the manuscript. J. C. and H. C. collected the data. Y. Z. and H. Z. analysed the data. X. H. edited the manuscript. W. M. and Z. X. provided conceptual advice.

Competing Interest: The authors declare no competing interest.

Tables

Parameter	No.
Sex	
Male	20 (62.5)

Female	12 (37.5)
Age (years)	
Range	19-80
Mean	49.09
Standard deviation	16.89
Epidemiological history	
Lived in or had travelled to Wuhan	10 (31.25)
Exposure to infected patient	17(53.13)
Unknown exposure	5 (15.62)
Symptoms	
Fever	27 (84.38)
Cough	19 (59.38)
Fatigue	5 (15.63)
Headache	6 (18.75)
Muscle soreness	3 (9.38)
Nausea	5 (15.63)

Table 1. Patient Clinical Features (N=32). Note: Results are represented as n (%) except Age.

Laboratory characteristics	Normal Range	Normal	Above Normal	Below Normal
White blood cell count ($\times 10^9$/L)	3.5-9.5	27 (84.4)	0 (0)	5(15.6)
Neutrophil count ($\times 10^9$/L)	1.8-6.3	30 (93.8)	1 (3.1)	1(3.1)
Lymphocyte count ($\times 10^9$/L)	1.1-3.2	12 (37.5)	0 (0)	20 (62.5)

Table 2. Patient Laboratory Characteristics (N=32). Note: Results are represented as n (%) except Normal Range.

Findings	No.
Pulmonary Lesions	
Location	
Unilateral	6 (20)
Bilateral	24 (80)
No. of Lobes Involved	
< 2	6 (20)
≥2	24 (80)
Frequency of Lobe Involvement	
Right upper lobe	19 (63.3)
Right middle lobe	15 (50)
Right lower lobe	24 (80)
Left upper lobe	21 (70)
Left lower lobe	27 (90)
CT Lung Severity Score	
Mean	4.72
Range	0-19
GGO	
Presence	30 (100)
Absence	0 (0)
GGO with Irregular Intralobular Lines	
Presence	26□86.7□
Absence	4□13.3□
GGO Morphology	

Round	25 (83.3)
Flaky	11 (36.7)
Semilunar	6 (20)
GGO and Consolidation	
Presence of either GGO or GGO with consolidation	30 (100)
Presence of GGO without consolidation	27 (90)
Presence of GGO with consolidation	23(76.7)
Presence of consolidation without GGO	0(0)
Distribution	
Peripheral region with/without Central region	30 (100)
Central region only	0 (0)

Table 3. Initial Abnormal CT Finding (N=30). Note: Results are represented as n (%) except CT lung severity score . GGO=ground-glass opacities.

	CT Lung Severity Score		Number of Lobes Involved	
	Correlation coefficient (*r*)	*P* Value	Correlation coefficient (*r*)	*P* Value
White Blood Cell Count	-0.135	0.460	-0.197	0.281
Lymphocyte Count	-0.363	0.041	-0.367	0.039

Table 4. Correlation between CT Data and Laboratory Data. Note: All data were analyzed by using the Pearson correlation test.

Figures

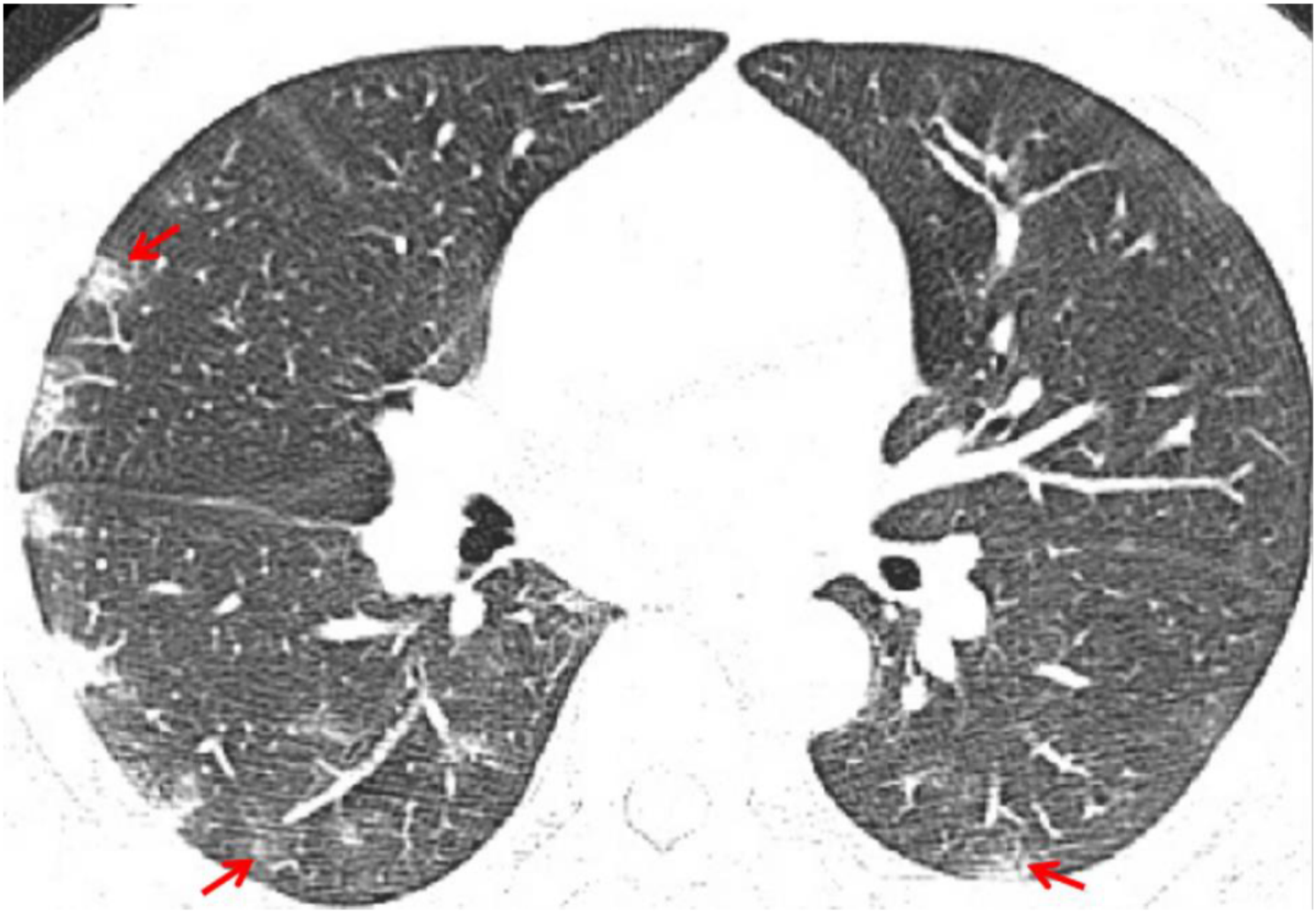

Figure 1

Image in a 47-year-old male with unknown exposure history of COVID-19 patients, presenting with fever and cough. Axial non-contrast HRCT CT image shows multiple bilateral ground-glass opacities with consolidation with a peripheral distribution (red arrows).

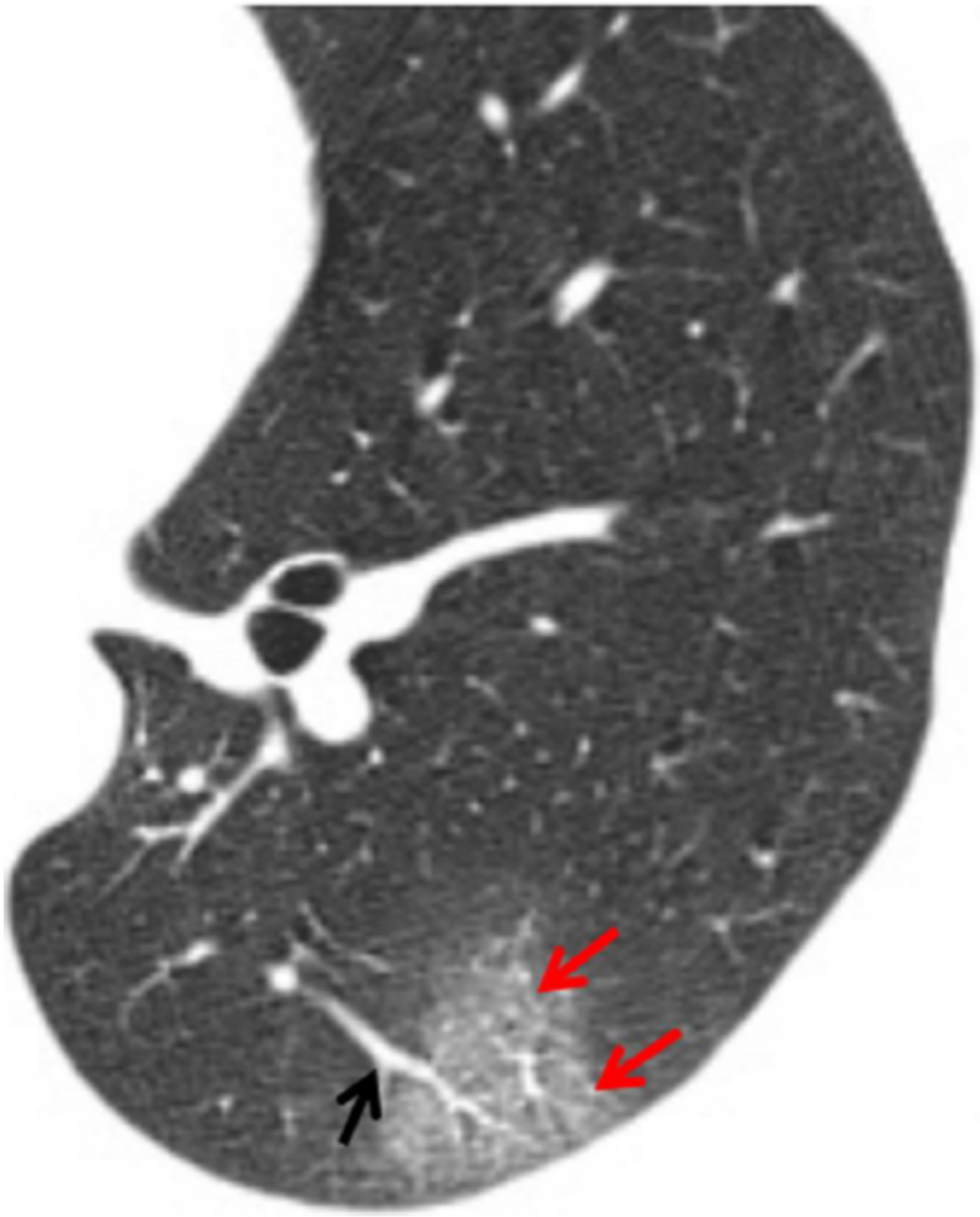

Figure 2

Image in a 43-year-old male having travelled to Wuhan, presenting with fever and headache. Axial non-contrast HRCT CT image shows vascular bundles congestion (black arrow) and irregular intralobular lines (red arrows) within a round ground-glass opacity.

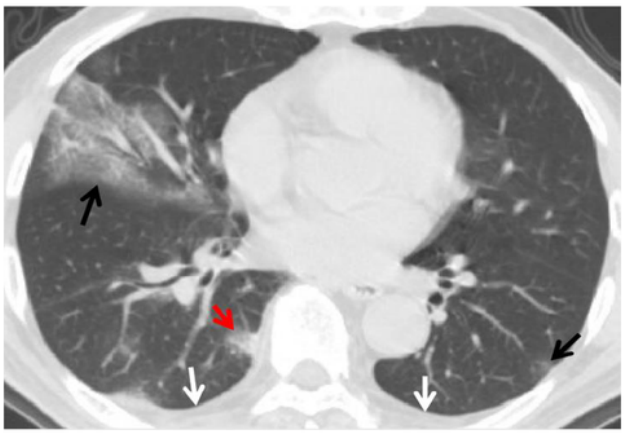

Fig. 3a

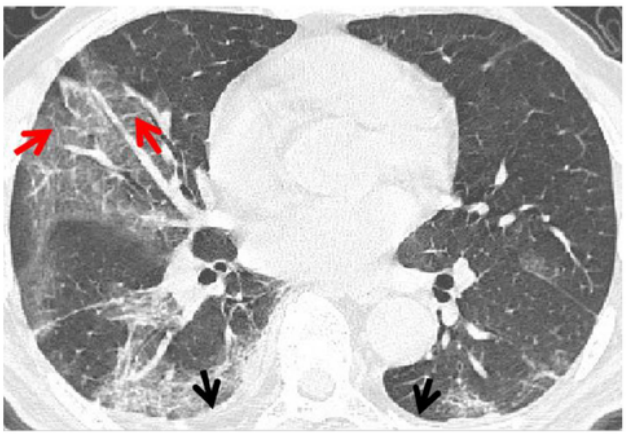

Fig. 3b

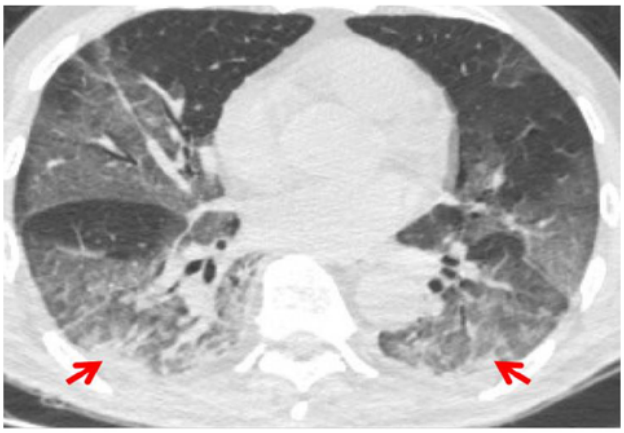

Fig. 3c

Figure 3

Images in a 75-year-old male living in Wuhan, presenting with fever and fatigue. (a) Axial non-contrast HRCT image (1/17/2020) shows multiple bilateral ground-glass opacities (black arrows) and banded consolidation (red arrow) with bilateral small amount of pleural effusion (white arrows). (b) Axial non-contrast HRCT image (1/19/2020) shows that the ranges of multiple bilateral pulmonary lesions increased. Numerous irregular intralobular lines (red arrows) are visible within the ground-glass opacities.

Bilateral pleural effusion is seen (white arrows). (c) Axial non-contrast HRCT image (1/21/2020) shows enlarged and increased ground glass opacities accompany with more solid areas (red arrows) in bilateral lungs, hinting disease progression.

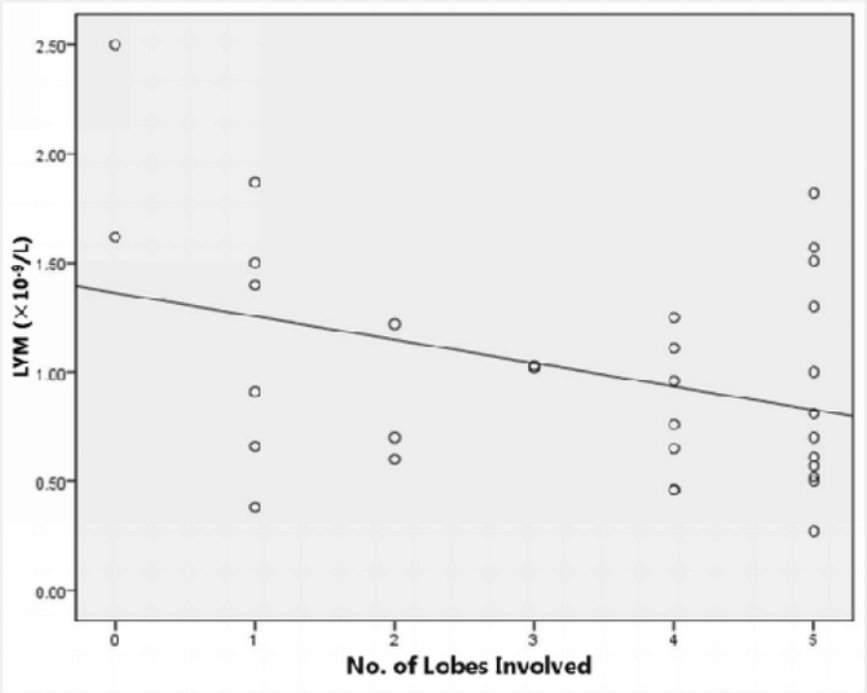

Fig. 4a

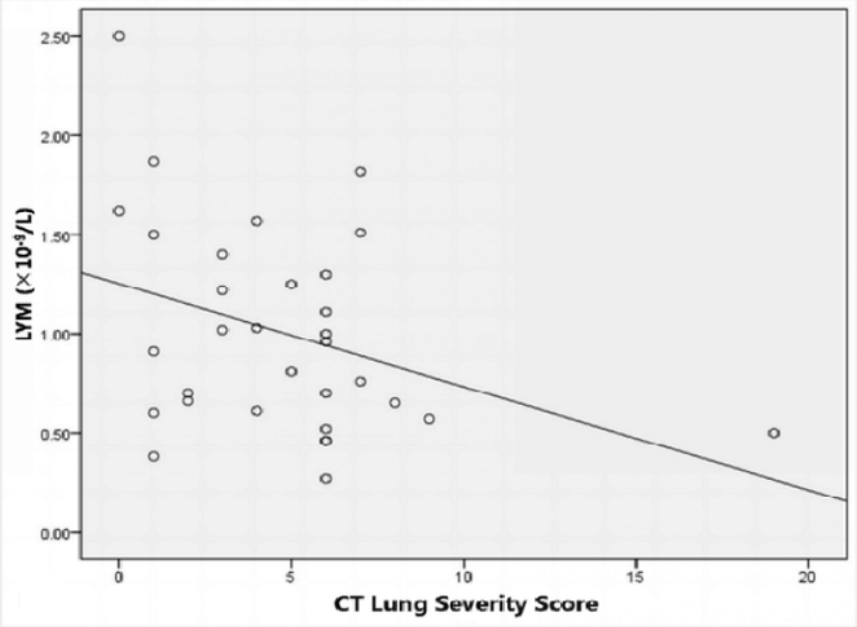

Fig. 4b

Figure 4

Scatter plots revealing correlation between CT data and lymphocyte count. (a) There is a negative correlation between the number of lobes involved and the lymphocyte count(r=-0.367, P=0.039). (b) This

scatter diagram demonstrates a negative correlation between the CT lung severity score and the lymphocyte count(r=-0.363, P=0.041).